Direct Electrochemical Conversion of the Chemical Energy of Raw Waste Wood to Electrical Energy in Tubular Direct Carbon Solid Oxide Fuel Cells

Magdalena Dudek[1] and Robert Socha[2]

[1]AGH – University of Science and Technology, Faculty of Fuels and Energy 30-059 Cracow, Poland
E-mail: potoczek@agh.edu.pl
2 Jerzy Haber Institute of Catalysis and Surface Chemistry Polish Academy of Sciences
Niezapominajek 8 30-239 Cracow, Poland

Raw wood chips from beech and acacia were chosen as a source of solid carbon fuels for utilization in tubular solid oxide fuel cells. These materials are typical wood waste products from carpentry in Poland. The physicochemical properties of carbon particles produced *in situ* during the operation of tubular direct carbon oxide fuel cells were determined by different analytical methods. It was found that solid carbon fuel had possessed high carbon content. Based upon structural investigations (X-ray diffraction analysis, Raman spectroscopy), it was found that disordered carbon or highly defected particles had been formed from raw waste wood during the operation of the fuel cell. No products of possible chemical reactions between carbon solid carbon fuel, or evaluated gases and nickel-ceria anodes, were observed during the start-up and operation of the DC-SOFC. It was found through electrochemical investigations that the power output of the DC-SOFC in question was ca. 100 mW/cm^2 at 800°C, which was similar to the performance of a DC-SOFC supplied with activated charcoals. A proposal of the construction of a small stack of tubular solid oxide fuel cells fed with biochar-based fuel was mentioned.

Keywords: direct carbon solid oxide fuel cells, carbon, wood waste products, biochar

1. INTRODUCTION

Biomass has many advantages compared to fossil fuels. One of the key benefits of this type of fuel is the absence of CO_2 omissions (when only the combustion process is taken into account and its production, treatment and transportation to the boiler is excluded) [1,2]. In addition to environmental aspects on a global scale, replacement of fossil fuels with renewable energy sources is of great social importance. Increasing the share of renewable energy in the European and global fuel and energy

balance contributes significantly to improvements in the efficient use and conservation of energy resources and to environmental improvement [3,4]. Biomass is generally used for energy purposes, both in its original form in the processes of direct combustion and co-combustion with coal and when processed in the form of liquid or gas. The direct combustion of biomass with an economically and environmentally acceptable level of energy efficiency, however, requires the use of appropriate technical solutions [5,6].

In the last decade there has been growing interest in the application of bio-carbon as a solid fuel for utilisation in fuel cell technology. The direct carbon fuel cell directly converts the chemical energy of carbon-based fuel into electricity without a reforming process. Potential sources of carbon, including coal, coke, graphite, municipal solid waste (MSW), activated charcoal, and carbon fibre derived from biomass such as rice hulls, nut shells, corn husks, grass and wood, all seem to be promising solid fuels for direct carbon fuel cells [7–10].

Direct carbon solid oxide fuel cell technology (DC-SOFC) is believed to be the most promising due to its uncomplicated construction and maintenance. In the case of DC-SOFCs [11-13], carbon can be directly electrochemically oxidised to CO_2 (according to equation 1):

$$C + O^{2-} \rightarrow CO_2 + 4e^- \tag{1}$$

as well as formed in a sequence of the following electrochemical reactions, (2) and (3):

$$C + O^{2-} \rightarrow CO + 2e^- \tag{2}$$

$$CO + O^{2-} \rightarrow CO_2 + 2e^- \tag{3}$$

The Boudouard reaction (4), involving CO_2 and C as reactants, is an additional source of CO consumed in reaction (3):

$$C + CO_2 \rightarrow CO \tag{4}$$

Direct solid oxide fuel cells usually operate at temperatures between 700–900°C. The most frequently applied solutions are electrolyte or anode-supported solid oxide fuel cells. Lesser power densities are obtained from DC-SOFCs at lower temperatures, usually not exceeding 120–180 mW/cm^2 at a temperature of 850°C [14].

The development of direct carbon fuel cells also opens up new opportunities for the chemical conversion of various carbonaceous fuels to produce electricity. Moreover, even certain raw and waste organic biomass materials and by-products from industrial processes appear to be suitable for conversion in DCFCs. Thus, new branches of chemical technology could be developed for the utilisation of certain solid organic materials which do not lend themselves to the technological recycling process [15,16].

Tubular direct carbon solid oxide fuel cells (DC-SOFCs) also appear to be an adequate solution for the construction of an efficient energy generator which will produce electricity cleanly. In DC-SOFCs, sealing problems seem to be less difficult than in the case of planar construction; moreover, these cells possess more favorable thermomechanical properties. Because of their excellent thermal shock resistance, the start-up/shutdown process is significantly faster than in planar cells [17,18]

As well, tubular solid oxide fuel cells offer simpler system concepts for continuous fuelling. In this field of technology, two options for solid fuel location can be considered. In one option, solid carbon powder fills the interior of a ceramic tube fabricated from a solid oxide electrolyte. The inner wall of the electrolyte (tube) is covered with a layer of the anode material and the outer with a layer of

the cathode material. In the second option, solid oxide fuel cells are placed in an outer container filled with solid carbon powder. In this method, the anode, placed on the outer wall of the electrolyte tube, is in direct contact with the carbon fuel. The cathode material is placed on the inner electrolyte wall. Either a solid fixed or a fluidized solid carbon bed can be applied in tubular solid oxide fuel cell technology [19,20].

R. Liu [21] investigated the tubular construction of a DC-SOFC fed with carbon black. The obtained value of power was approximately 100 mW/cm^2. Y. Bai et al. [22] demonstrated the potential for the construction of a short stack of direct carbon solid oxide fuel cells. Tubular cone-shaped Ni-based anode-supported solid oxide fuel cells (SOFCs), each with a yttria-stabilised zirconia (YSZ) electrolyte and a $La_{0.8}Sr_{0.2}MnO_3$ (LSM) cathode, were tested. A 3-cell stack, with segmented cone-shaped cells connected in series, was assembled and tested. A peak power density of 465 mW /cm^2 and a volumetric power density of 710 mW/cm^2 were achieved at 850°C.

These results demonstrate the feasibility of the direct conversion of carbon to electricity in tubular solid oxide fuel cell technology.

The aim of this paper was to present the potential for the utilisation of raw waste wood as a solid fuel for a DC-SOFC operating with a tubular configuration

2. ANALYTICAL METHOD OF CARBON EVALUATION

Raw wood chips from beech and acacia were chosen as a source of solid carbon fuels which can be formed during DC-SOFC start-up and operation within a temperature range of 25–1000°C. These materials are typical waste products from wood used in carpentry in Poland. To estimate how much solid carbon powder could be obtained from beech and acacia wood in the course of thermal heating at 850°C for 24 h in argon gas flow, several samples were pyrolysed in a gas-tight quartz reactor in the specified conditions.

The efficiency of bio-carbon production was estimated by weighing the biomass before and after the carbonisation process.

The phase compositions of all the carbon samples thus obtained were evaluated by X-ray diffraction analysis (XRD) with reference to the ICDD database. The content of carbon (C) and sulphur (S) in all the investigated samples were determined with a PerkinElmer 2400 CHN Elemental Analyzer.

Chemical surface analyses of the carbon fuels were performed using the XPS/ESCA method with a hemispherical analyser (Gammadata Scienta SES R4000). The spectra were processed with CasaXPS 2.3.12 software, while the background was estimated using a Shirley profile. Deconvolution of spectra into a minimum number of components was done using the application of Voigt-type line shapes.

Raman studies were carried out using a Horiba Jobin Yvon LabRAM HR micro-Raman spectrometer equipped with a CCD detector. An excitation wavelength of 532 nm was used, with a beam intensity of about 10mW. Acquisition time was set at 30 seconds.

Scanning electron microscopy (Nova NanoSEM), coupled with an EDS system, was used to characterise the morphology and chemical composition of the carbon particles.

Thermal effects occurring during the heating of the solid carbon fuel within the temperature range 25–1000°C in argon gas flow were measured by the DTA/DSC and TG methods (TA Instruments SDT 2960). The samples (ca 50 mg) were ramped up at a rate of 10 K·min^{-1} in an alumina crucible.

The impact of gaseous and liquid products originating from the decomposition of organic and inorganic compounds included in the raw wood chips was determined, as was the effect of solid biocarbon particles on the thermal and chemical stability of the electrolyte and anode materials. Electrolytes made of 8 %mol Y_2O_3 in ZrO_2 (8YSZ) and covered with Ni-10GDC film were placed in an alumina crucible and then into a gas-tight quartz reactor heated in a coal bed at 850°C for 300 h under argon flow as the shielding gas. After being cooled to room temperature while the gas flow was shielded, the experimental samples were withdrawn from the reactor and analysed.

2.1 Electrochemical investigations of carbon particles oxidation

The direct electrochemical oxidation of carbon was studied in tubular solid oxide fuel cell C|Ni-10 GDC|8YSZ|LSM-10GDC|LSM|O_2 (1)

The schematic design of DC-SOFC is presented in Fig. 1.
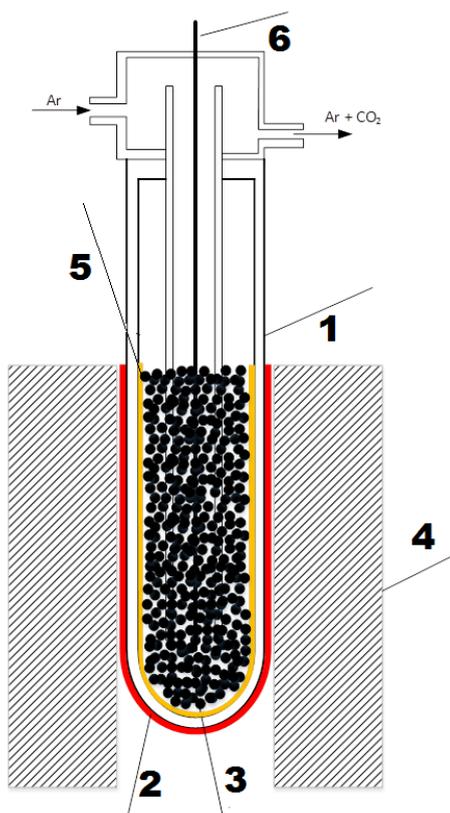
Figure 1. The tubular direct carbon solid oxide fuel cell: 1- Electrolyte 8YSZ, 2- cathode LSM, 3- Ni-GDC, cermetallic anode material, 4 – electric furnace, 5 – solid fuel

A single conventional one-end-closed electrolyte-supported solid oxide fuel cell was used. The solid oxide electrolyte used was a tube of 8 % mol Y_2O_3 in ZrO_2 (8YSZ).

The thickness of the 8YSZ electrolyte was about 1.1 mm. LSM is a $La_{0.8}Sr_{0.2}MnO_3$ cathode material; 10GDC denotes a ceria-gadolina solid solution, 5 %mol Gd_2O_3 in CeO_2. Ni-GDC is also a cermetallic anode consisting of 50 %vol nickel particles distributed in a GDC matrix. Raw wood as a source of solid carbon powder was put into the bottom of one YSZ tube covered with Ni-GDC anode materials. Gold wires were used as current collectors. Electrochemical measurements were performed within a temperature range of 500–850°C, using a PGSTAT 300N potentiostat equipped with GPES (chrono and pulse techniques) and FRA (electrochemical impedance spectroscopy) modules. In the course of the measurements, Ar was used as a shielding gas introduced to the anode chamber.

3. RESULTS

The typical biochar yield from raw wood materials after thermal treatment at 850°C for 24 h in an argon gas atmosphere does not exceed 30 %wt. The high values of mass losses observed during experiments can be attributed to a large amount of volatile matter, which is characteristic for solid fuels involving biomass.

Chemical analysis of the total carbon as well as sulphur of carbon-based powder originating in raw wood will help to determine its potential as a solid fuel in DC-SOFC technology. Analysis of all parameters collected in Table 1 indicate that charcoal-based samples produced in a reactor as well as *in situ* in a DC-SOFC during operation are characterised by high concentrations of carbon, estimated about 84–86 wt%. This content is similar to commercially available charcoal samples previously tested in DC-SOFCs, indicating that solid carbon-based powder produced *in situ* appears to be a valuable solid fuel for this application.

Table 1. The carbon and sulphur concentration in solid fuels analyzed, (wt.%)

Solid fuel	C	S
A	86.7	0.02
B	83.8	0.03

X-ray diffraction analysis (Fig. 2) showed that powders obtained from pyrolysed trees are monophase charcoal-based samples. The investigated charcoal sample showed two broad peaks in the ranges 10−30° and 30−60°, which are known to be characteristic of poorly crystalline carbon particles. These peaks indicate that the obtained charcoal is characterised by a short-range graphite-like (or turbostratic) structure. The considerable contribution of disordered carbon particles is a promising feature for its utilisation as a solid fuel in DC-SOFCs.
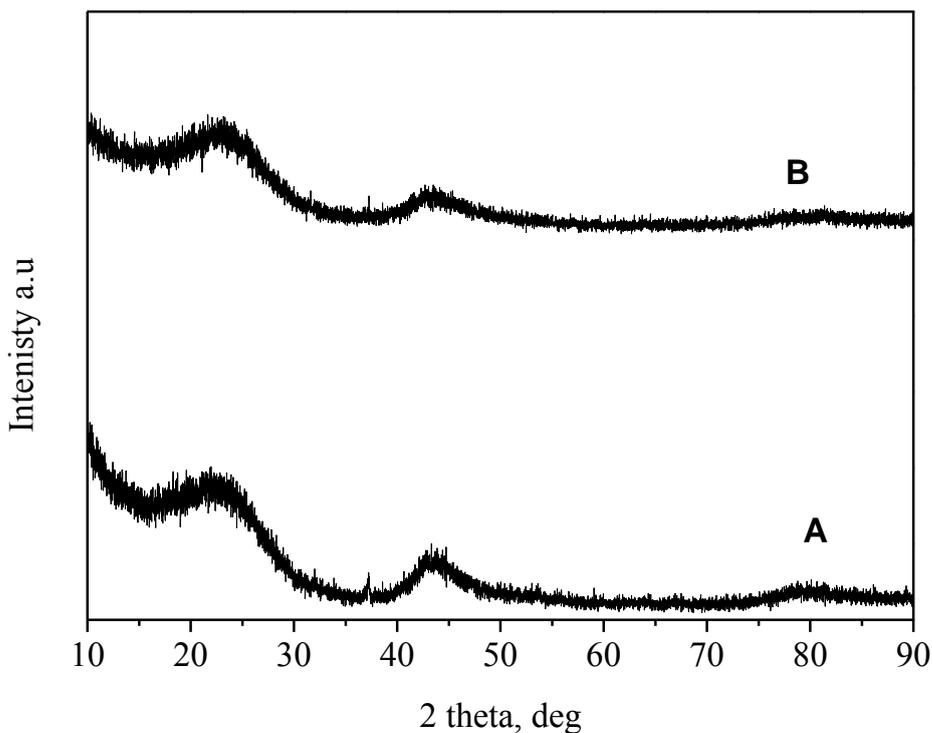
Figure 2. The XRD diffraction pattern recorded for carbon-based fuels originating from beech wood (A) or acacia wood (B)

Raman spectroscopy was applied as an analytical technique complementary to XRD in order to elucidate the structural properties of the carbon materials, with special emphasis put on the presence of graphite in the samples. The Raman spectrum of fuel A and B is shown in Fig. 3.
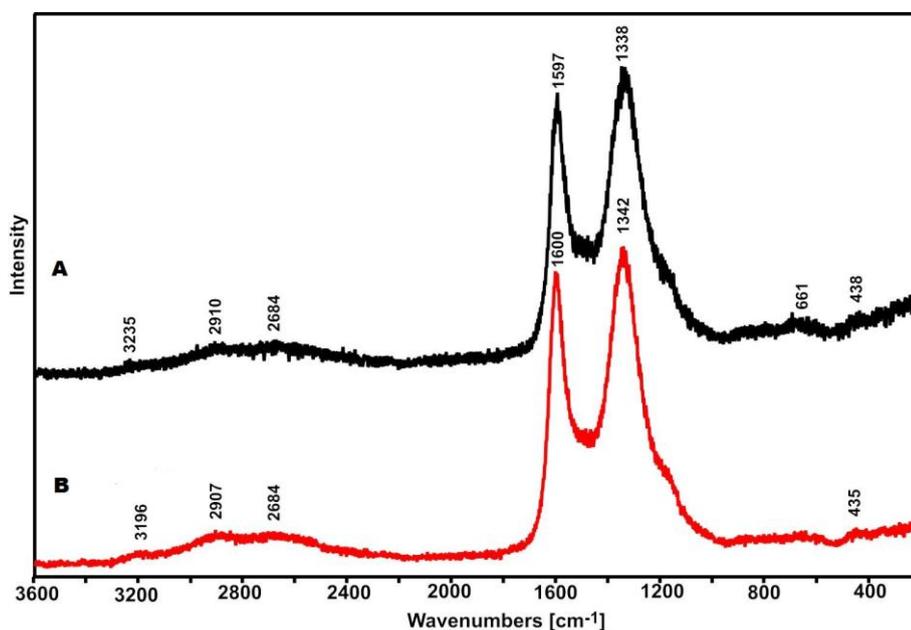

Figure 3. Raman spectra recorded for carbon-based fuels originating from beech wood (A) or acacia wood (B)

The spectrum reveals distinctly visible G (ca 1580 cm^{-1}) and G′ (ca 2680 cm^{-1}) bands, along with one at 2910 cm^{-1} which is a combination of D and G, thus confirming the existence of sp^2, characteristic for graphite structures. Simultaneously, the presence of strong D-bands at 1345 cm^{-1} and 660 cm^{-1} suggests an amorphous carbon phase. This material consisted of particles of highly defected graphite phases as well as some rather disordeded carbon phases. It was previously found that the presence of highly disordered carbon particles in solid fuel enhances the electrochemical oxidation of carbon particles in a DC-SOFC [23,24].

The XPS analysis allowed us to determine atomic compositions and electronic properties of the elements present at the surface of charcoal particles. The analysis was performed for the surface layer up to the depth of 10.3 nm. The surface composition of the analyzed charcoal was presented in Table 2. The table showed that the particles were slightly oxidized and oxygen to carbon ratio was 0.064. The total amount of metal traces approached 1.2 at.%.

Table 2. The XPS determined elemental composition of the charcoal particle surface (at.%).

C	O	P	Cl	N	S	Si	Ca	K	Co	Mg
92.1	5.9	0.2	0.1	0.1	0.1	0.3	0.5	0.4	0.1	0.2

The high resolution C 1s core excitation (Fig.4a), showing graphite-like envelope, was deconvoluted into six components assigned to specific carbon species.
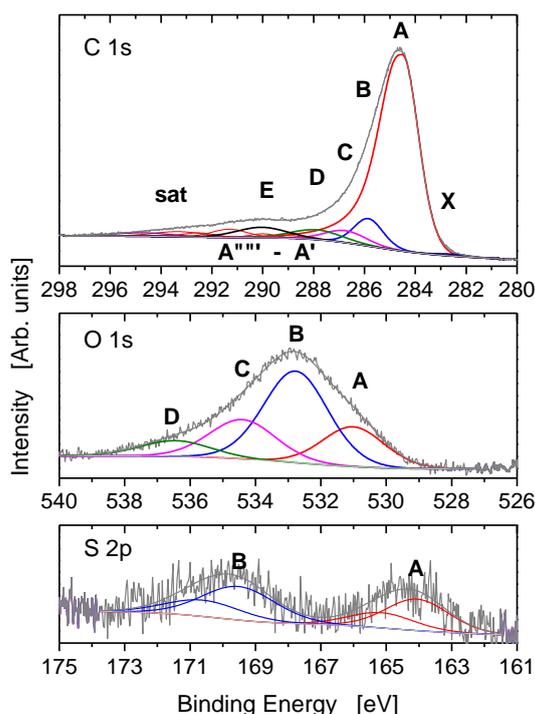

Figure 4. The deconvolution of C $_{1s}$ (a) , O $_{1s}$ (b) and S $_{2p}$ (c) core excitations.

The main carbon component was fitted with the asymmetric peak associated with five satellites ascribed to plasmon and dipole excitations according to the procedure described by Leiro et al [25].

The parameters of the C 1s spectrum components and their assignations [26,27] were collected in Table 3.

Table 3. The parameters of the deconvoluted C 1s, O 1s and S 2p spectra.

Excitation	Component	BE [eV]	FWHM [eV]	%	Assignation
C 1s	X	282.6	1.5	0.5	Carbides
	A	284.5	1.5	78.3	C-C sp^2
	B	285.8	1.4	7.3	C-C sp^3
	C	286.7	1.9	4.5	C-O, C-N, C-S
	D	287.9	2.3	4.5	C=O, O-C-N, O-C-S
	E	290.0	2.3	4.8	COOH + CO$_3^{2-}$ + C-Cl
	A'-A'''''	288.9-293.3	1.2-2.3	-	plasmon and dipole excitation satellites
	sat	294.7	2.6	-	π^* shake-up
O 1s	A	531.0	2.2	20.5	OH
	B	532.8	2.3	48.7	H$_2$O + O^{2-} in aliphatic compounds
	C	534.4	2.4	21.7	O^{2-} in aromatic compounds
	D	536.4	2.5	9.1	O^{2-} in cyclic hydrocarbons + π^* shake-up
S 2p$_{3/2}$	A	164.1	2.3	44.8	organic sulphur
	B	169.5	2.6	55.2	Sulfates

The main spectrum component (A) was assigned to sp^2 carbon whereas the second one (B) to sp^3 carbon. The sp^2/sp^3 ratio was 10.7 suggesting that graphite-type carbon is main charcoal surface component. On the other hand, low amounts of oxidized carbon species (components C-E) were also found at the analysed surface. These results could be confirmed by rather low level of oxidant (O, N, P, Cl) contaminations (Tab. 2) that is rather related to aromatic systems than aliphatic. The presence of peak X at electron binding energy lower than for elemental carbon suggested metal-carbon bonding in the sample.

The O 1s spectrum (Fig. 4c) was deconvoluted into components assigned to oxygen in hydroxyl groups (component A) or oxygen in water or aliphatic compounds (B) or oxygen in aromatic (C) or cyclic compounds and shake-up satellites of π^* electrons (D) (Table 3).

The main component of O 1s excitation was assigned to oxygen in aliphatic compounds confirming larger oxidation of aliphatic carbon species. It is worth noticing that the O 1s line corresponds to a nonspecific excitation, where several components can show similar BE at the maximum of the photoelectron spectrum. It can be also postulated that the responses attributed to the oxygen components are related to the presence of adsorbed water in the samples. The S$_{2p}$ spectrum was

deconvoluted into two doublets (Tab. 3 and Fig.4c) showing that slightly more than half of sulphur species (B) were in the form of sulphates whereas the rest (A) were in the form of organic sulphur.

Thermal analysis of the samples was performed in order to elucidate the thermal processes that took place while heating the samples to temperatures of DC-SOFC operation, i.e. 600–1000°C. Typical DTA/DSC-TG curves recorded for wood chips and acacia wood are presented in Fig. 5a–b during heating and argon flow.

a)

b)
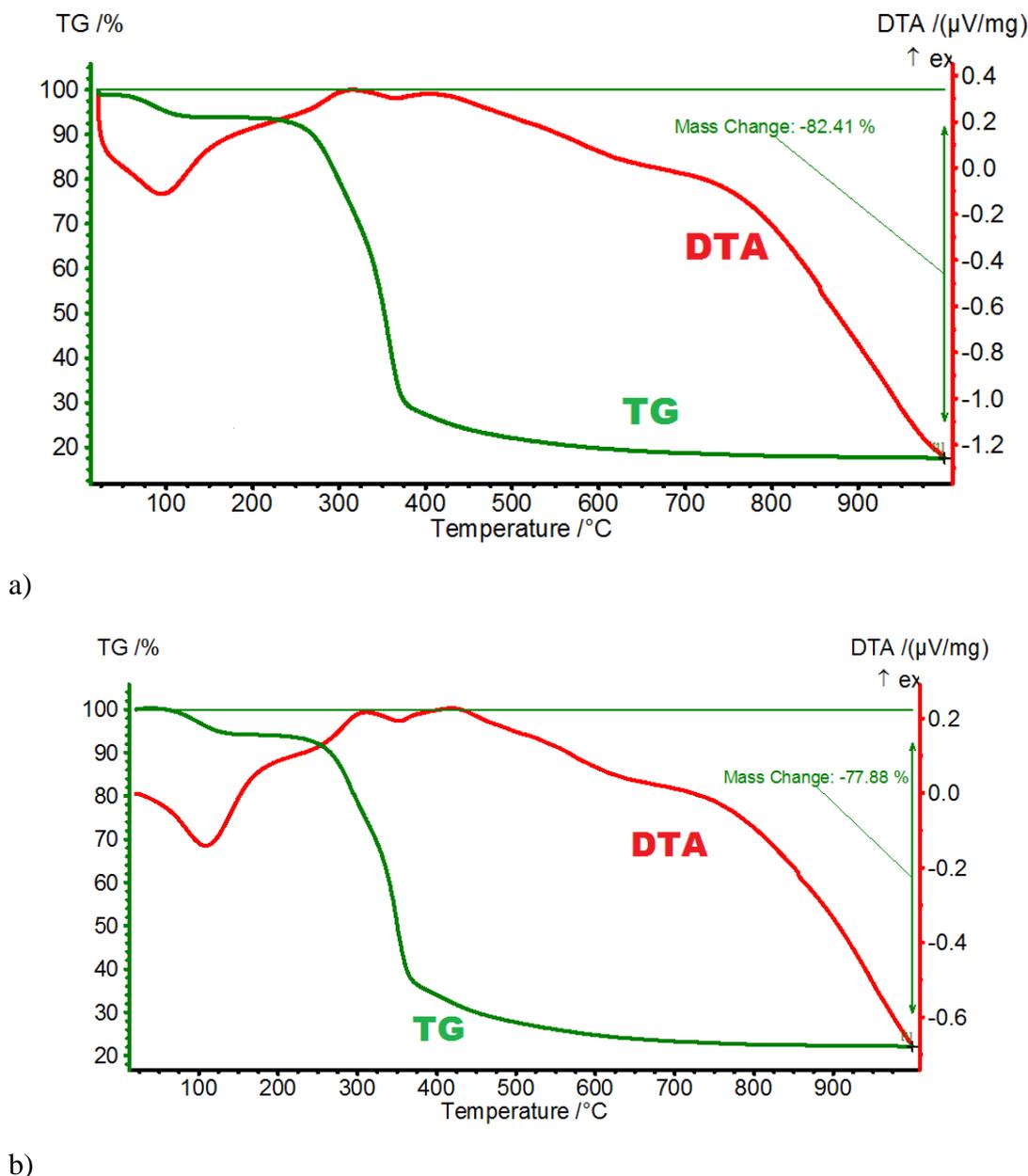
Figure 5. The DTA-TG curves recorded for carbon-based fuels originating from beech wood (a) and acacia wood (b)

Analysis of DTA and TG curves indicated that the first thermal effect observed in DTA curves near 100°C was water evaporation. An additional endothermic effect was observed up to 500°C. In the case of these samples, losses of about 30% and 60% were recorded at 400°C.

Some thermal effects originating in pyrolysed samples were detected in the temperature range 300–500°C. For temperatures higher than 600°C, no thermal effects corresponding to phase changes were observed. These results clearly indicated that, at temperatures typical for direct solid oxide fuel cell operation, pure carbon solid fuel should be obtained. Considerable mass losses of about 80 wt% were observed based on TG analysis.
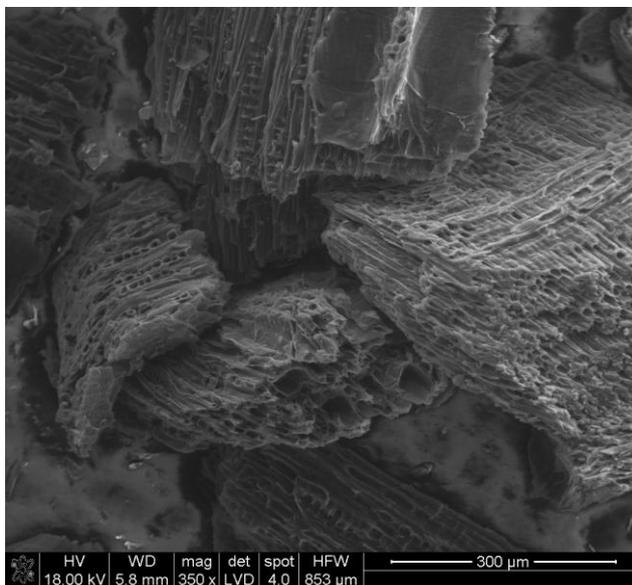

Figure 6a. SEM microscopy of carbon particles originating from raw beech wood (A) during DC-SOFC operation.
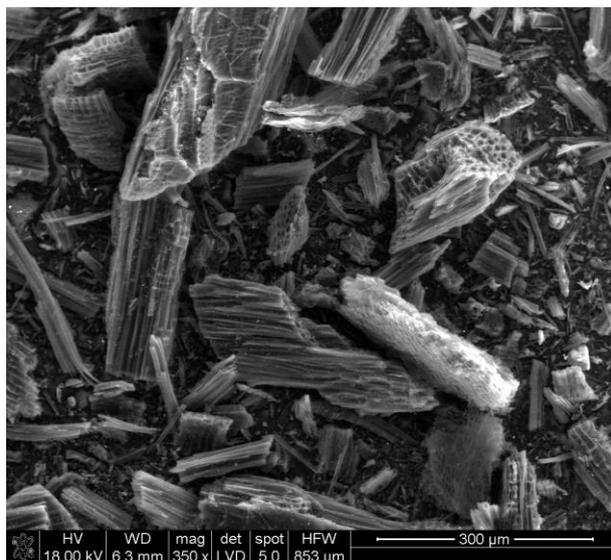
Figure 6b. SEM microscopy of carbon particles originating from raw acacia wood (B) during DC-SOFC operation

In the case of DC-SOFC operation, morphology, particle sizes and pore structures are especially important parameters determining performance. It was previously found that an effect is exerted by the morphology of graphite powders on the electrochemical oxidation of carbon particles Analysis of family curves ΔE-I recorded for a DC-SOFC supplied with needle graphite particles showed very low current densities in comparison to those obtained from the same DC-SOFC supplied with isometric carbon particles [26]
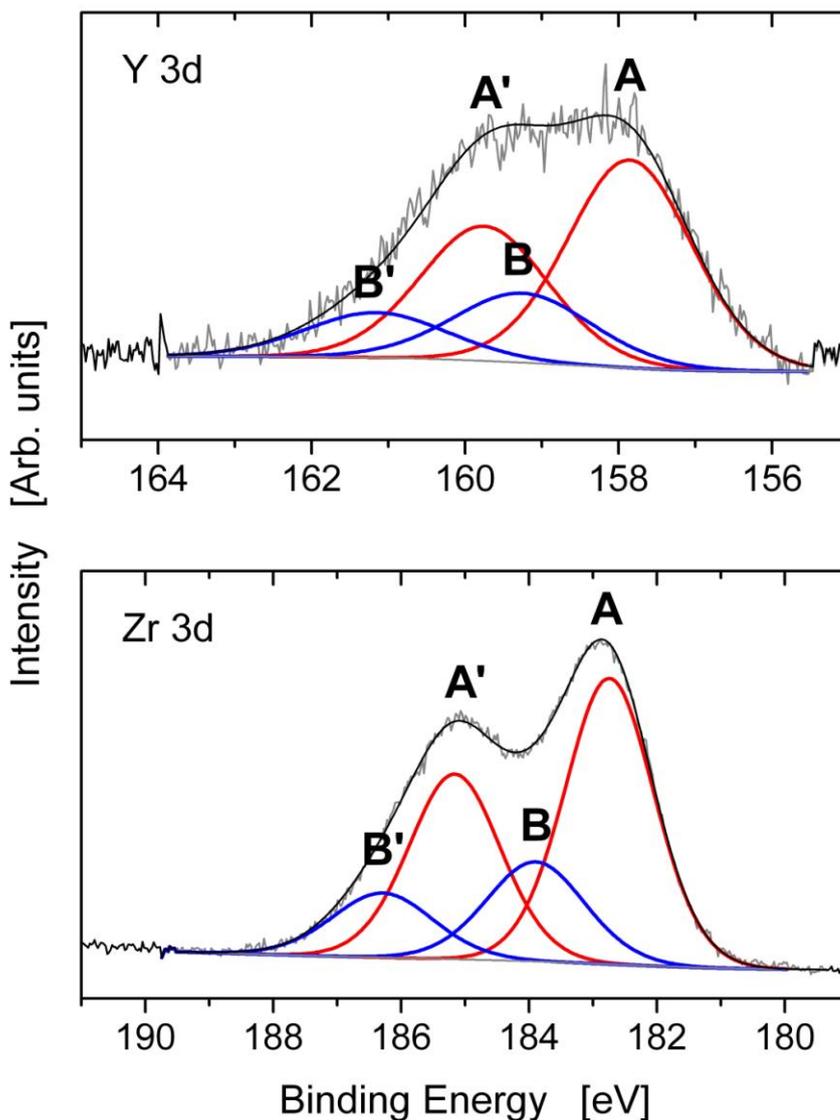
Figure 7. The deconvolution of Y, Zr core excitations.

The problem of choosing an adequate carbon type as a source of fuel for DC-SOFC technology is further complicated by a limited reaction zone in the solid state, restricted to direct contact between carbon particles and the surface of solid oxide electrolytes or anode materials.

Typical SEM microphotographs of carbon (A) and (B) particles are presented in Fig. 6a–b.

As observed, carbon (A) consists mainly of isometric particles with dimensions ranging from 100 to 350 μm. In the case of carbon particles obtained from acacia band (B), the dimensions of some needle-shaped particles range from 50 to 300 μm.

Among the main requirements are the thermal and chemical stability of cell components during start-up, thermal cycling, and operation over a long period of time. There must be no corrosion products from carbon particles, nor gases evaporated during waste wood pyrolysis.

X-ray diffraction and XPS analysis indicated no considerable changes in the chemical composition of the Ni-GDC anode as well as 8YSZ or 10GDC solid solutions as a possible product of the chemical reaction between such components and gaseous products evaporated during pyrolysis in the DC-SOFC. No additional phases were found as possible products of chemical reaction also between solid carbon and anode or 8YSZ material.

XPS analysis (Fig.7) also enabled us to determine the atomic compositions and electronic properties of the elements present on the surface of charcoal particles adsorbed on the 8YSZ electrolyte surface. A considerable amount of carbon was observed on the 8YSZ surface, along with Si, P, and Ce impurities, following the joint heating of raw biomass samples and the 8YSZ electrolyte.

Small amounts of silica and phosphorium were detected on the surface of the 8YSZ electrolyte – in the case of Si, in the form of silica (bonding energy, BE Si 2p3/2 = 102.2 eV). Additionally, deconvolution of the Zr 3d as well as the Y (3d) spectrum enabled us to determine that Y^{3+} was present in Y_2O_3 or in chemical bonds with organic matter. The contribution of B″ may be related to a possible reaction between (Y-O) and carbon under the applied conditions. A similar situation was observed in the analysis of the Zr 3d spectra. Zr^{4+} was detected in ZrO_2 solid solution as well as A: Zr^{4+} and B: Zr^{4+} in connection with OH groups or organic matter. A high BE value was indicated for B in the reaction f Zr^{4+} with oxidated organic matter.

Neither analysis of SEM observation of the surface of Ni-GDC (Fig.8 a-b) nor a cross section of the investigated SOFC cell indicated any degradation on the surface of anode materials or delamination of the anode from the 8YSZ electrolyte.
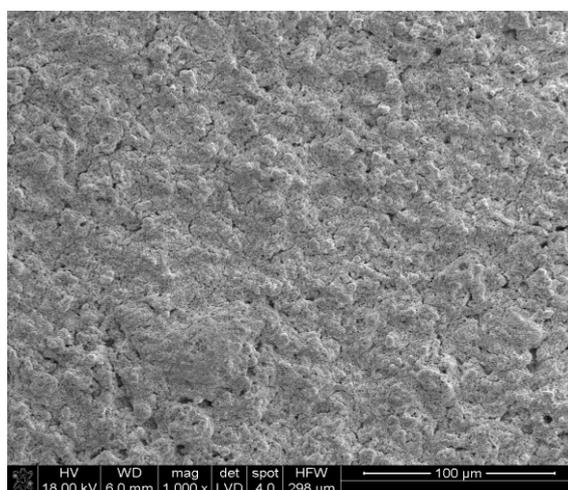

A
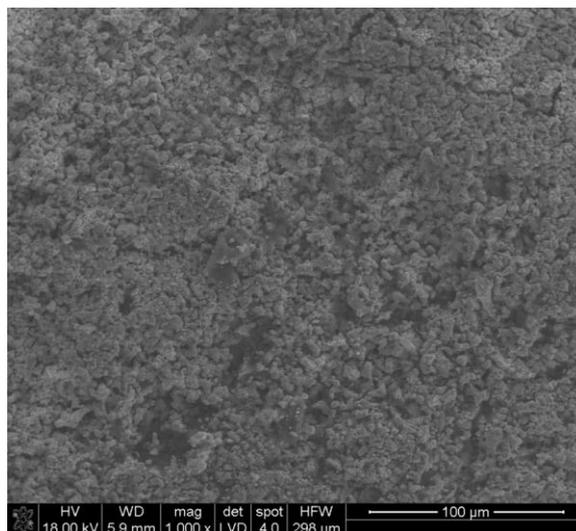
B

Figure 8 a-b. The SEM observation of Ni-GDC anode surface before and after thermal tests

Typical dependencies of voltage (ΔE) vs current density (I) and power density (P) vs current density (I) at various operating temperatures for a type TDC-SOFC with a Ni-GDC cermetallic anode are shown in Fig. 9.

The ΔE vs I characteristics of the fuel cell were determined using a slow cyclic linear voltammetry method at a scan rate of $v = 5$ mV/s. These experiments were performed under argon flow supplied to the anodic compartment of the cell. The raw beech and acacia were used as solid fuels
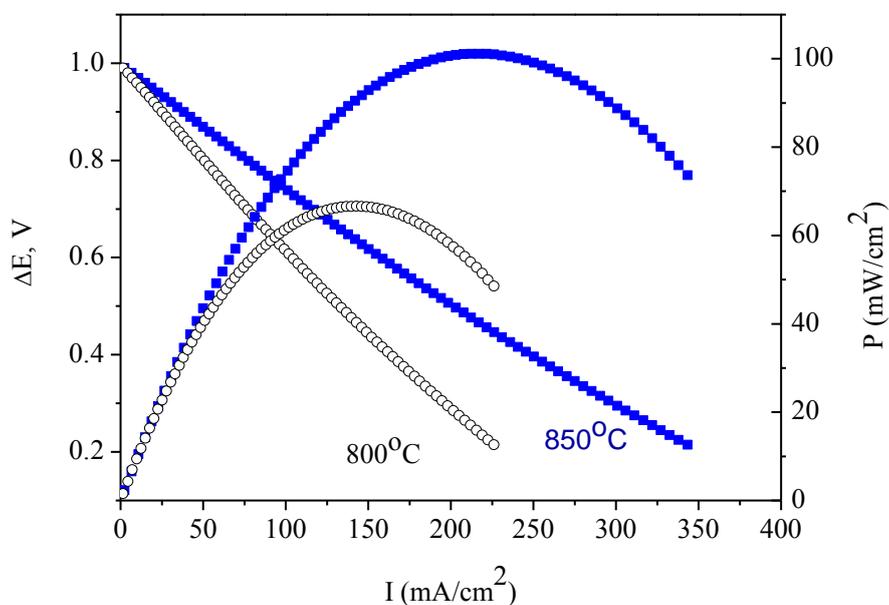
A
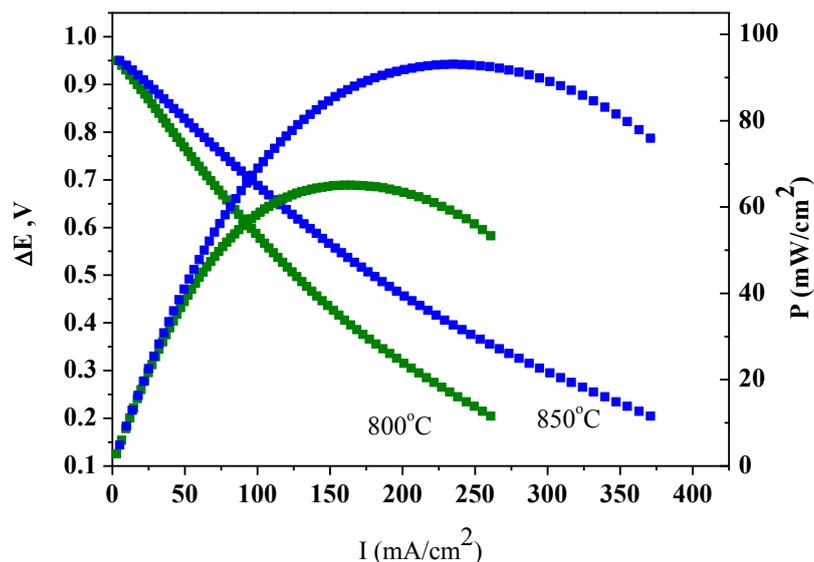
B

Figure 9. Family of ΔE-I and P-I curves recorded for DC-SOFC fed with raw beech a) and b) acacia wood

The current and power densities were determined using the geometric area of the anode for a fuel cell with tubular geometry. The obtained values of current and power density acquired from TDC-SOFC fed with raw beech are close to those obtained for commercial charcoal. The typical performance of a DC-SOFC varies from 60 to 110 mW/cm^2. The direct comparison of DC-SOFC fed with raw beech chips compared to acacia chips showed a similar performance.

Finally, we examined the behaviour of a DC-SOFC (Fig.10) fed with raw wood during a prolonged operation. The tests were performed at 800°C for 300 h under load ΔE =-0.5V.

As can be seen, a continuous small decrease was observed. This fact could be probably attributed to a decrease in disordered carbon particles, which are consumed firstly during electrochemical oxidation of carbon particles and the further slow-electrochemical oxidation of graphite particles occurred. The difficult gas outlet from this construction of a tubular direct carbon fuel cell also have some negative impact on the performance over a long period of time. It was found that siring solid particles during DC-SOFC operation facilitates the outlet of gases from the anode chamber. This resulted the increase of power output of such fuel cells.

Further work, apart from improving performance, could be related with the construction of a DC-SOFC stack operating with chracoal solid fuel. Trials using DC-SOFCs with a tubular electrolyte were carried out during this stage of the process. The structure of the stack is relatively simpler, and does away with modules, as the issue is the thickness of walls available on the oxygen electrolyte market, which cause a high loss of power density consumed from cells due to high ohmic polarization. A diagram of the stack composed of two cells is presented in Fig.11.
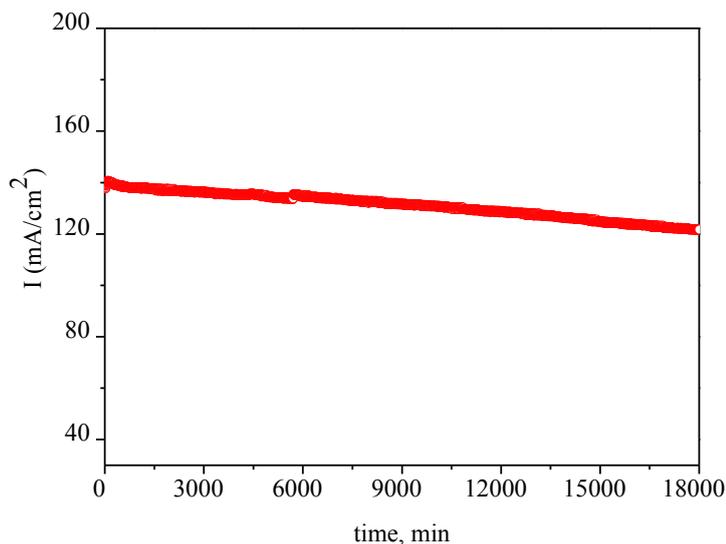
Figure10. The TDC-SOFC operation under load ΔE= -0.5V at 800°C. The raw beech chips were used
as fuel
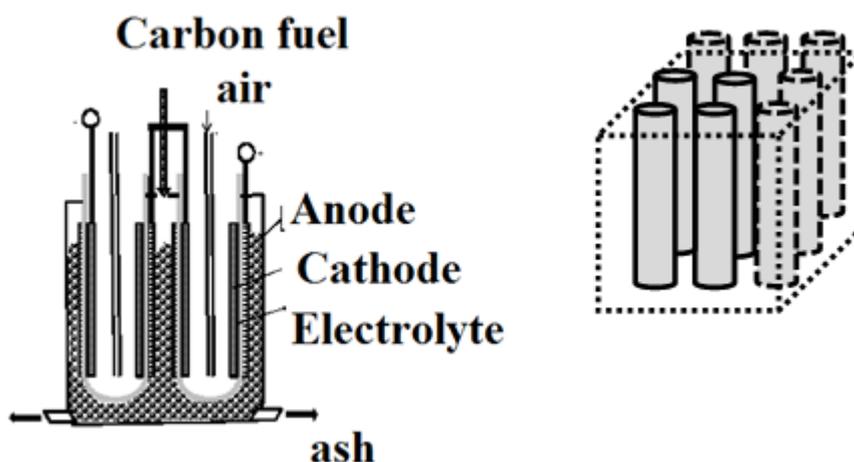
Figure 11. The proposal of construction of the short tubular solid oxide fuel cell stack fed with biochar

Its developing construction leads to adding more cells to the system. Carbon fuel is placed in the container, which simultaneously is the external casing for the stack. Carbon fuel is in direct contact with anodes of the cells (situated on the external walls of tubular electrolyte). The air is fed to the interior of tubular electrolytes where the cathodes are situated. On the basis of obtained data, it safe to assume that the power of the DC-SOFC based on the tubular electrolyte 300 mm in length, wall thickness of ca. 1.5 mm, internal diameter of 8 mm, amounts to ca. 0.5 W. This means that constructing a stock with a power rating of ca. 10 W will need to use ca. 20 tubular fuel cells with the dimensions given above.

4. CONCLUSION

The waste wood chips formed in situ during the DC-SOFC start up and operation seem to be promising solid fuels for DC-SOFC application.

It was found that solid carbon fuel possess high carbon content (84 % wt), which is similar to typical commercial samples. Based upon structural investigations (X-ray diffraction analysis, Raman spectroscopy) it was found that disordered carbon particles or mostly defected graphite particles are formed during fuel cell operation. No products of possible chemical reactions between carbon solid carbon fuel or evaluated gases and nickel –ceria anodes were observed during such conditions. Based upon electrochemical investigations it was found that the power output of the investigated DC-SOFC was about 110 mW/cm^2 at 800°C, which was similar to performance of the DC-SOFC supplied by activated charcoals. It is believed that elaborating on methods of choppering wood can led to improving the performance of a DC-SOFC. The second idea was improving the gas outlet from an anode chamber during DC-SOFC operatiion. The proposition of constructing DC-SOFC stacks was also presented.

References

1. J. M. Joelsson, L.Gustavsson, *Biomass Bioenerg* 7 (2010) 967,
2. K. Möllersten, J. Yan, J. R. Moreira *Biomass Bioenerg* 25 (2003) 273,
3. P. Carneiro, P. Ferreira, *Renew Energ*, 44 (2012) 17
4. N. Kautto, P. Peck, *Renew Energ* 46 (2012) 23
5. M. M. Roy, K. W. Corscadden, *Appl Energy* 99 (2012) 206
6. D. Maraver, A. Sin, J. Royo, F. Sebastián, *Appl Energy* 102 (2013)1303
7. A. Dicks, *J Power Sources* 156 (2006)128
8. M.Dudek, P.Tomczyk, R.Socha, J. Jewulski, M.Skrzypkiewicz, *Int. J.Electrochem.Sci* 8(2013)3229-3253
9. S.Y.Ahn, S.Y. Eom, Y.H.Rie, M.Y.Soung, Ch.E. Moon, G.M.Choi, D.J. Kim, *Energy* 51 (2013) 447
10. S. L.Jain, Y. Nabae, B.Lakeman, K.Pointon, J.Irvine, *Solid State Ionics* 179 (2008) 1417
11. X. Yu, Y. Shi, H. Wang, N. Cai, Ch.Li, R. Tomov, J. Hanna, B.A. Głowacki, A. Ghoniem,
a. *J Power Sources* 243 (2013) 159,
12. A. Kulkarni, S. Giddey, S.P.S. Badwal, *Solid State Ionics* 194 (2011) 46
13. M.Dudek, P.Tomczyk, R.Socha, M. Hamaguchi, *Int. J. Hydrogen Energy* 39 (2014)12386,
14. S. Giddey, S.P.S. Badwal, A. Kulkarni, C. Munnings, *Prog. Energy Combust. Sci.* 38 (2012) 360
15. C. Jiang, J. T.S. Irvine, *J Power Sources* 196 (2011) 7318,
16. M. Dudek, P. Tomczyk, K.L. Juda, R.Tomov, B.A.Glowacki, S. Batty P. Risby, R.Socha *Int. J. Electrochem. Sci.*7 (2012) 6704
17. S.L. Jain, J.B. Lakeman, K.D. Pointon, R. Marshall and J.T S. Irvine, Electrochemical performance of a hybrid direct carbon fuel cell powered by pyrolysed MDF, *Energy Environ. Sci* 2 (2009) 687
18. A. D. Bonaccorso, J.T. Irvine, *Int. J. Hydrogen Energy* 37(2012) 19337

19. T. M. Gür, *J. Electrochem. Soc*. 157 (2010) B571
20. A. C. Lee, S. Li, R. E. Mitchell, and T. M. Gür, *Electrochem. Solid State Lett*. 11 (2008) B20
21. 21.R. Liu, Ch. Zhao, J. Li, F. Zeng, S.Wang, T.Wen, Z. Wen *J Power Sources* 195 (2010) 480
22. Y. Bai, Y.Liu, Y. Tang, Y.Xie, J.Liu *Int. J. Hydrogen Energy* 36 (2011) 9189
23. M. Dudek, M. Sitarz, P.Tomczyk, *J. Solid State Electrochem.* (2014) in print
24. P.Desclaux, H.C.Schirmer, M. Woiton, E.Stern, M.Rzepka, *Int. J.Electrochem.Sci* 8 (2013) 9125 – 9132
25. J.A. Leiro, M.H. Heinonen, T. Laiho, I.G. Batirev, *J. Electron Spectrosc. Relat. Phenom.* 128 (2003) 205–213
26. J. F. Moulder, W. F. Stickle, P. E. Sobol, and K. Bomben (J. Chastain, editor), Handbook of X-ray Photoelectron Spectroscop 2nd ed. Perkin-Elmer Corporation (Physical Electronics), 1992 (2nd edition).
27. NIST X-ray Photoelectron Spectroscopy Database; http://srdata.nist.gov/xps/

/